NANO LETTERS
Cite This: Nano Lett. 2020, 20, 577−584
Letter
pubs.acs.org/NanoLett

Dynamic Manipulation of Cell Membrane Curvature by Light-Driven Reshaping of Azopolymer

Selene De Martino,[†,‡,§] Wei Zhang,[§] Lasse Klausen,[§] Hsin-Ya Lou,[§] Xiao Li,[§] Felix S. Alfonso,[§] Silvia Cavalli,[†] Paolo A. Netti,[†,‡] Francesca Santoro,[*,†] and Bianxiao Cui[*,§]

[†]Center for Advanced Biomaterials for Healthcare, Istituto Italiano di Tecnologia, Largo Barsanti e Matteucci, 53, 80125 Napoli, Italy

[‡]Dipartimento di Ingegneria Chimica dei Materiali e della Produzione Industriale, DICMAPI, Università degli Studi di Napoli Federico II, Piazzale Tecchio, 80, 80125 Napoli, Italy

[§]Department of Chemistry, Stanford University, 333 Campus Drive, Stanford, California 94305, United States

Supporting Information

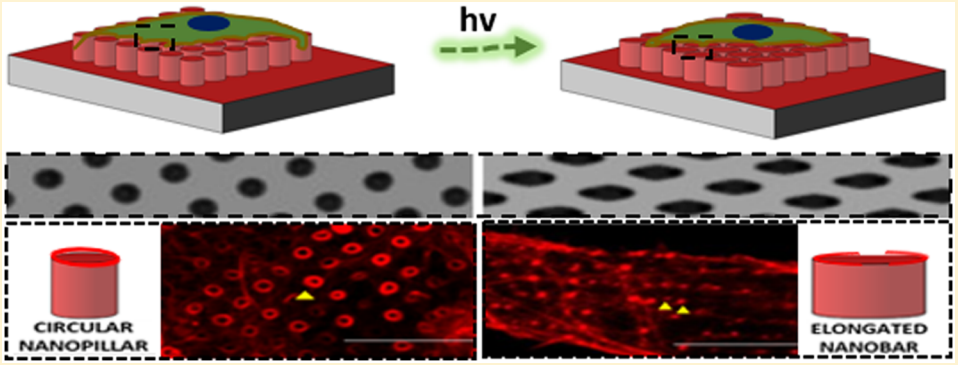

ABSTRACT: Local curvatures on the cell membrane serve as signaling hubs that promote curvature-dependent protein interactions and modulate a variety of cellular processes including endocytosis, exocytosis, and the actin cytoskeleton. However, precisely controlling the location and the degree of membrane curvature in live cells has not been possible until recently, where studies show that nanofabricated vertical structures on a substrate can imprint their shapes on the cell membrane to induce well-defined curvatures in adherent cells. Nevertheless, the intrinsic static nature of these engineered nanostructures prevents dynamic modulation of membrane curvatures. In this work, we engineer light-responsive polymer structures whose shape can be dynamically modulated by light and thus change the induced-membrane curvatures on-demand. Specifically, we fabricate three-dimensional azobenzene-based polymer structures that change from a vertical pillar to an elongated vertical bar shape upon green light illumination. We observe that U2OS cells cultured on azopolymer nanostructures rapidly respond to the topographical change of the substrate underneath. The dynamically induced high membrane curvatures at bar ends promote local accumulation of actin fibers and actin nucleator Arp2/3 complex. The ability to dynamically manipulate the membrane curvature and analyze protein response in real-time provides a new way to study curvature-dependent processes in live cells.

KEYWORDS: *Azopolymer, topography, nanobio interface, light-stimuli materials, F-actin, dynamic biointerface*

Many studies show that nanoscale 3D structures significantly affect cell adhesion, migration, proliferation, and stem cell differentiation.[1,2] A few examples include nanopillars enhancing osteogenic differentiation of mesenchymal stem cells (MSCs)[3,4] and inhibiting cell migration,[5,6] nanogratings and nanopores inducing cell alignment[7−9] and differentiation of stem cells,[10−13] and nanoroughs modulating macrophage activity.[14,15] At the cellular level, the presence of 3D nanostructures locally changes the curvature of the plasma membrane, which affects curvature-dependent intracellular processes such as endocytosis[16,17] and actin dynamics.[18−22] When cells are in contact with 3D structured surfaces, their cell membranes deform to wrap around these structures. The resulting membrane curvatures act as biochemical signals to activate intracellular curvature-dependent proteins and underly 3D structure-induced regulation and tuning cell behavior.[19] For example, our recent study shows that 3D nanostructures promote actin polymerization in a curvature-dependent manner and are mediated by a curvature-sensing protein FBP17.[23]

Previous studies of topographic effect on cell behavior use prefabricated and static 3D structures.[21,23−28] Although these structures were very useful in identifying curvature-dependent

Received: October 18, 2019
Revised: December 9, 2019
Published: December 17, 2019

DOI: 10.1021/acs.nanolett.9b04307
Nano Lett. 2020, 20, 577−584

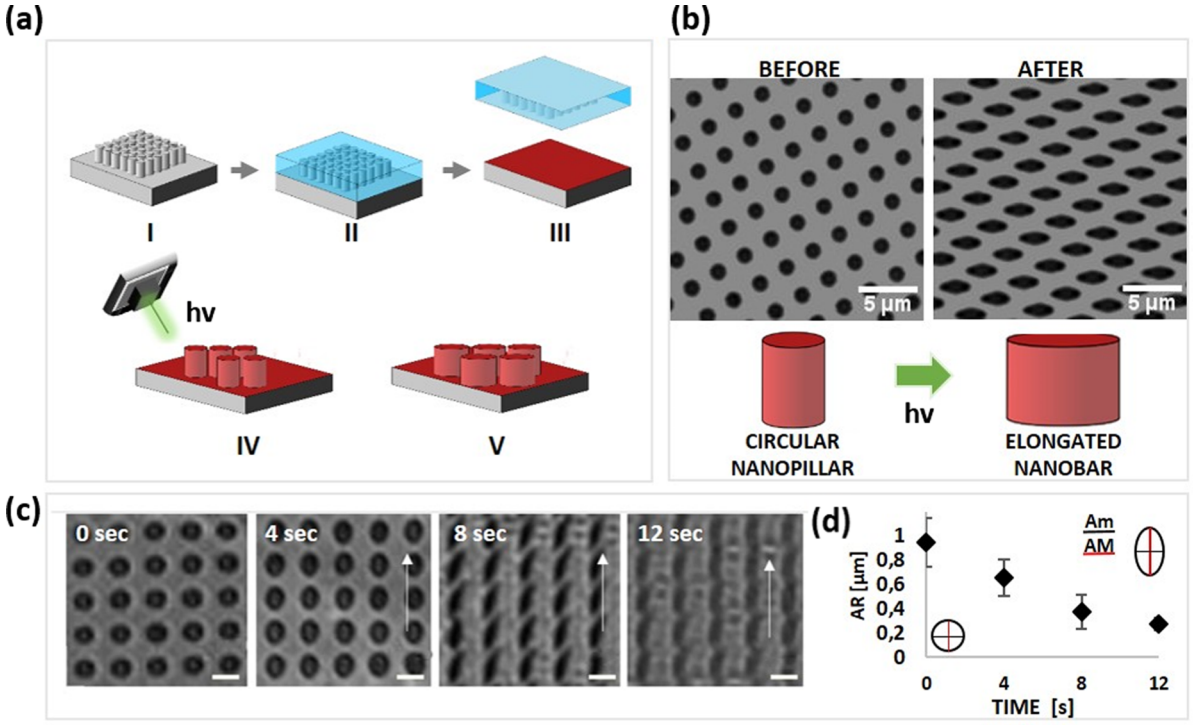

Figure 1. Light-induced reshaping of azopolymer 3D structures. (a) Schematics of azopolymer pillar fabrication and light induced shape deformation; (I) silicon master fabricated by e-beam lithography, (II) replica of the PDMS mold, (III) soft imprinting of the PDMS mold on a thin film of pDR1m azopolymer for making azopolymer pillars. Imprinted azopillar array (IV) can be reshaped into azobar array (V) after light illumination. (b) Brightfield images of azopolymer pillars before and after a green laser-induced deformation. Scale bar 5 μm. Lower part, schematic of single pillar-to-bar deformation by light illumination. (c) Bright-field images of polymer pillars at different exposure time. Pillar transit from pillar (0 s), to slightly elongated (4 s), to bar-like structures (8−12 s). Scale bar 2 μm. (d) Aspect ratio value (AR= Am/AM) for pillars during laser irradiation from 0 to 12 s. Minor axes (Am) are represented in black and major (AM) in red.

protein components and intracellular processes, their static nature means that membrane curvatures induced by these structures are also static. On the other hand, curvatures on the cell membrane appear and disappear dynamically in response to complex intracellular and extracellular cues. Smart materials with the ability to change their 3D shapes upon light stimulation would afford a new approach to manipulate membrane curvatures on-demand.[29−32]

In the last two decades, light-responsive materials such as azobenzene-based polymeric compounds have attracted significant interest as smart materials. The photoisomerization of azobenzene induces conformational changes of the polymer chains that in turn lead to modifications of the material physical and mechanical properties.[33] For example, a cyclic trans−cis−trans isomerization of azobenzene upon light exposure leads to a mass displacement of azopolymer either at the microscopic or macroscopic level along the polarization direction of the illumination beam.[34,35] The light-induced deformation of azopolymer has been demonstrated to cause significant shape changes when azobenzene-based polymers are made into 3D structures.[29,36,37] This process, referred as directional photofluidization lithography, has provided advances in the fabrication of complex micro and nano-architectures otherwise not easily fabricated by conventional methods.[38] Furthermore, light-induced deformation of azopolymer has shown to dynamically change material characteristics such as melting temperature, robustness, and surface wettability.[29,36,37,39−41]

In this work, we utilize light-driven reshaping of azopolymer to dynamically manipulate the geometry of 3D vertical nanostructures. The cell membrane is highly fluid and dynamic so that it easily adapts to mechanical perturbations. Previous work has shown that the cell membrane readily deforms when pushed or pulled by atomic force microscopy or optical tweezers.[42,43] Therefore, the cell membrane will change shape together with the azopolymer nanostructures upon green light illumination. Here, we show that light-driven reshaping of azopolymer nanopillars to nanobars in the presence of living cells dynamically imparts curvatures at the plasma membrane (PM). The induced membrane curvatures promote the formation of actin fibers at the locations of high curvature and accumulation of the actin nucleator Arp2/3 complex.[23,44] The ability to manipulate the membrane curvature on-demand and analyze cell response in real-time provides a new way to study how surface topography modulates cell behavior and intracellular processes.

Results. *Light-Induced Reshaping of Vertical Azopolymer Pillars.* Our substrates consist of well-ordered arrays of vertical micropillars made of pDR1m azopolymer, fabricated on glass coverslips by soft lithography (through a PDMS mold, which is replicated against a silicon master wafer) as shown in Figure 1a. The fabrication process of the silicon master by e-beam lithography allows for precise control over the pillar dimensions as well as the center-to-center distance (pitch) between pillars. The silicon master was inversely replicated into PDMS molds that were subsequently used as stamps for imprinting the azopolymer pillars. Under polarized light irradiation, the azopolymer of the same polarization absorbs photons, and the trans−cis isomerization induces an athermal transition of the glassy azopolymer into a fluid state. This

DOI: 10.1021/acs.nanolett.9b04307
Nano Lett. 2020, 20, 577−584

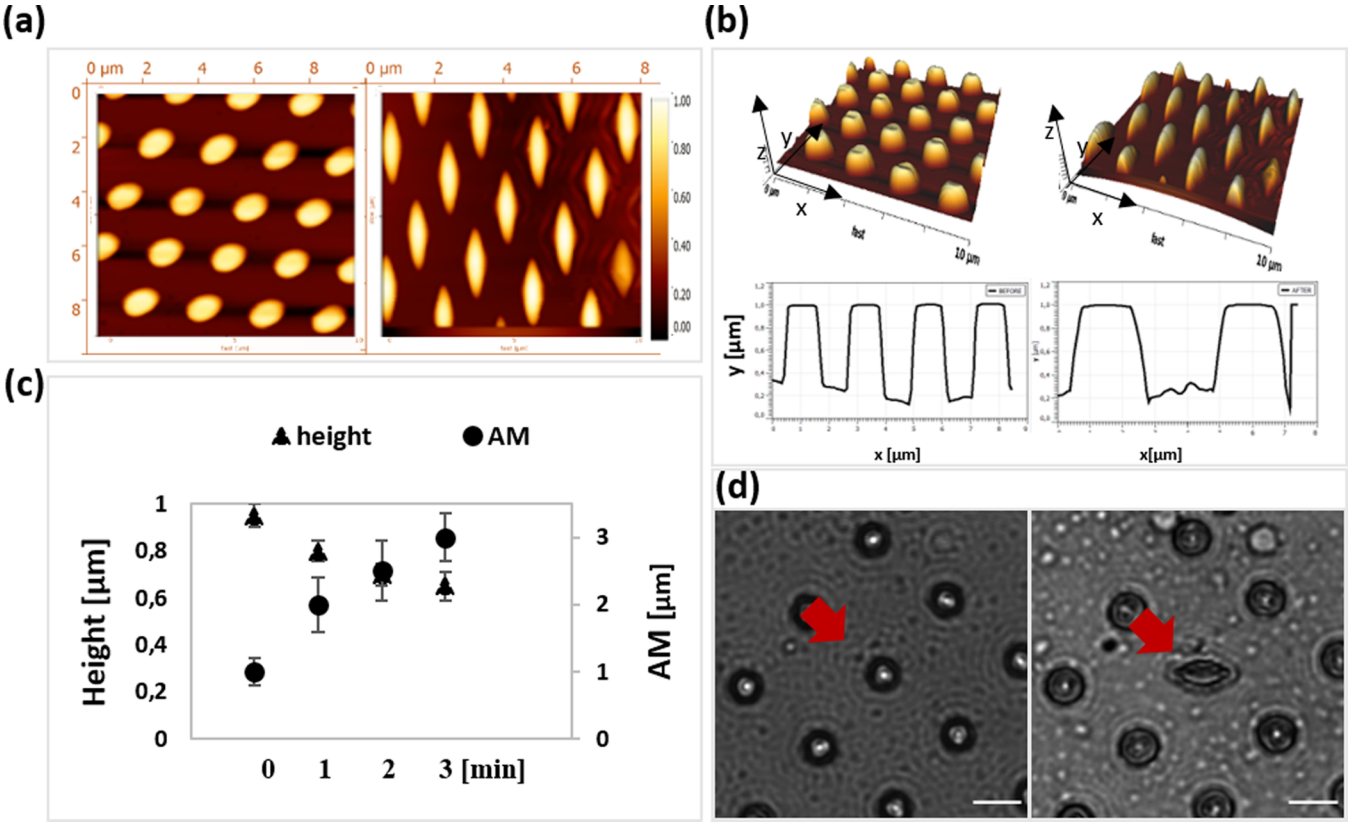

Figure 2. AFM characterization of light-reshaped individual azostructures. (a) AFM topographic images show the transformation of circular pillar (500 nm radius) arrays to elliptical bar arrays (3000 nm length in major axis) under a confocal microscope. (b) Three-dimensional AFM measurements and section profiles of azopillars and light-reshaped azobars. (c) Plot of height (triangle) and major axes length (circle) of elongated pillars over time (0−3 min). (d) Brightfield images of a single azopillar selectively reshaped by a 514 nm laser under a confocal microscope. A region of interest (ROI) is defined around the selected azopillar. Scale bar 10 μm.

induces a distinct mass migration along the direction of the light polarization and a shape transition from pillars to ellipsoidal bars.[41]

We first used a 532 nm CW linearly polarized solid state laser to illuminate a relatively large area of the substrate. The degree of deformation depends on the irradiation conditions such as wavelength, intensity, and exposure time.[45] Figure 1b shows the brightfield images of an azopolymer nanopillar array before and after 5 s of illumination by the 532 nm laser at 1.5 mW; the light exposure allows for the transition from circular nanopillars into elongated nanobars of the whole array. The deformation magnitude increases with the exposure time providing a shape progression from pillar to slight elongation, to a bar-like structure in 0, 4, 8, and 12 s, respectively (Figure 1c). In terms of effective nanostructures dimensions, here, the nominal initial nanopillars radius was 500 nm, and the interpillar distance was 1.5 μm. However, the newly shaped nanostructures have been characterized by the mean roundness defined as the aspect ratio (AR) between the minor (Am) and the major axis (AM) of the elongated bars. Here, we found that this ratio decreases almost linearly with the exposure time (Figure 1d). For our purpose, we chose a 5 s illumination, which gave the best results in terms of elongation and separation of azobars with an AR $\approx$ 0.5.

Light-induced deformation of azopillars can also be achieved using green light from a confocal microscope. Atomic force microscopy (AFM) was used to characterize the morphology of azostructures before and after confocal light illumination (Figure 2a). AFM measurements show the transformation of a cylindrical pillar (500 nm in radius) array to an elliptical bar array (3000 nm length in major axis) after 3 min illumination under a confocal microscope. The resulting profiles show that the ends of the elliptical bars are much narrower than the middle, with the width about 460 $\pm$ 50 nm. By changing the pillar section from circular to elliptical, we also induce a gradual change of the radius of curvature at the ends of azobars. As we show later, these ends are locations where the cell membrane has the highest curvature. AFM measurements of the 3D profiles reveal that these azopillars have vertical walls before light illumination (Figure 2b). The light illumination not only induced nanostructure elongation but also simultaneously induced a decrease in height and softening of the sidewalls (Figure 2c). Next, we demonstrated that it is possible to selectively control and tune the reshaping on individual azopolymer pillars by using a confocal microscope light at 514 nm. By scanning inside a region-of interest centered around a single azopillar, we selectively deformed the azopillar to the bar shape within an array of pillars (Figure 2d). This method can be used to modify locally a tension of a plasma membrane in a particular region of a single cell. Nevertheless, in this work, we focus on the reshaping of a large area of pillars to remodel the cell membrane's architecture of cell population.

Curvature-Dependent Actin Polymerization Can Be Induced by Light-Driven Reshaping of Azopolymer Structures. We first confirmed that azopillars and the reshaped azobars are compatible with live cell culture (Figure S1 in the Supporting Information), in agreement with previous reports on azopolymer biocompatibility.[29,46] To confirm that light-

DOI: 10.1021/acs.nanolett.9b04307
Nano Lett. 2020, 20, 577−584

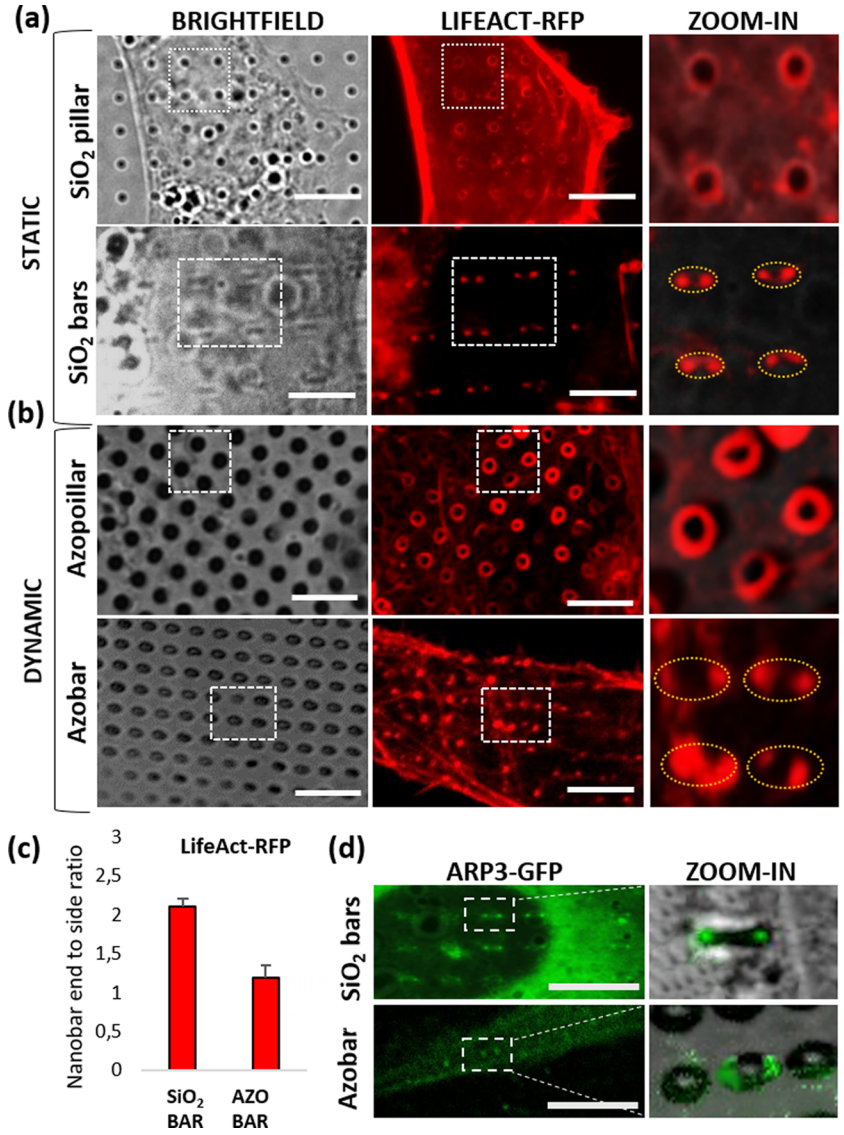

Figure 3. Azobars induce curvature-dependent actin polymerization. (a) Brightfield and fluorescence images of U2OS cells transfected with Lifeact-RFP on static SiO_2 structures. Lifeact-RFP appears as a ring around nanopillars and preferentially accumulates to the ends of SiO_2 bars. Scale bar 10 μm. (b) Brightfield and fluorescence images of U2OS cells transfected with Lifeact-RFP on azostructures. Similar to SiO_2 nanostructures, Lifeact-RFP appears as a ring around azopillars and appears as two spots at the ends of azobars. Scale bar 10 μm. (c) Quantification of nanobar end-to-side ratios for Lifeact-RFP on SiO_2 bars and azobars (n = 10 cells for each condition). Error bars represent s.e.m. (d) Fluorescence images of U2OS cells expressing Arp3-GFP show strong preference of Arp3-GFP to the ends of SiO_2 nanobars as well as azobars. Scale bar 10 μm.

driven reshaping of azopolymer structures is able to induce curvature-dependent intracellular responses, we probe the distribution of cellular fibrous actin (F-actin) in response to the presence of different 3D structures. Our recent studies show that static SiO_2 nanobar induces high membrane curvatures at its ends while relatively flat membrane along its side walls. F-Actin preferentially accumulates at the ends in correspondence of high membrane curvatures.[16,19] Here, cells were transfected with LifeAct-RFP for live-cell fluorescence imaging of F-actin. Static SiO_2 pillars (500 nm in diameter and 1 μm in height) and bars (200 nm in width, 2000 nm in length, 1 μm in height) nanostructures are used as positive controls. Live-cell imaging shows that F-actin forms a ring-structure around SiO_2 nanopillars but exhibits strong fluorescence signal at the ends of nanobars with much low signal along the sidewalls of nanobars (Figure 3a). The strong accumulation of F-actin at the end of SiO_2 nanobars confirms our recent observations that high membrane curvatures at the ends of nanobars induce local polymerization of F-actin.[18]

Furthermore, we observed that F-actin forms a ring-structure also around azopillars as shown in Figure 3b, while it shows strong accumulation at the two ends of light-reshaped azobars, a phenomenon similar to the accumulation of F-actin at the ends of SiO_2. This result demonstrates that light-reshaped azobars are indeed able to induce curvature-dependent F-actin formation similar to static SiO_2 nanobars. Quantification of the F-actin end-to-side ratios on bar structures shows that the preferential accumulation on the ends of azobars (1.21 $\pm$ 0.04) is less than that on SiO_2 nanobars (2.1 $\pm$ 0.1) (Figure 3c). This is due to the fact that the size of azobar ends (~400 nm) is much larger than that of SiO_2 nanobars (200 nm), which results in a lower curvature and less F-actin accumulation. Furthermore, it is worthy to note that the pillar height is reduced depending on the elongation state of the pillars, which

DOI: 10.1021/acs.nanolett.9b04307
Nano Lett. 2020, 20, 577−584

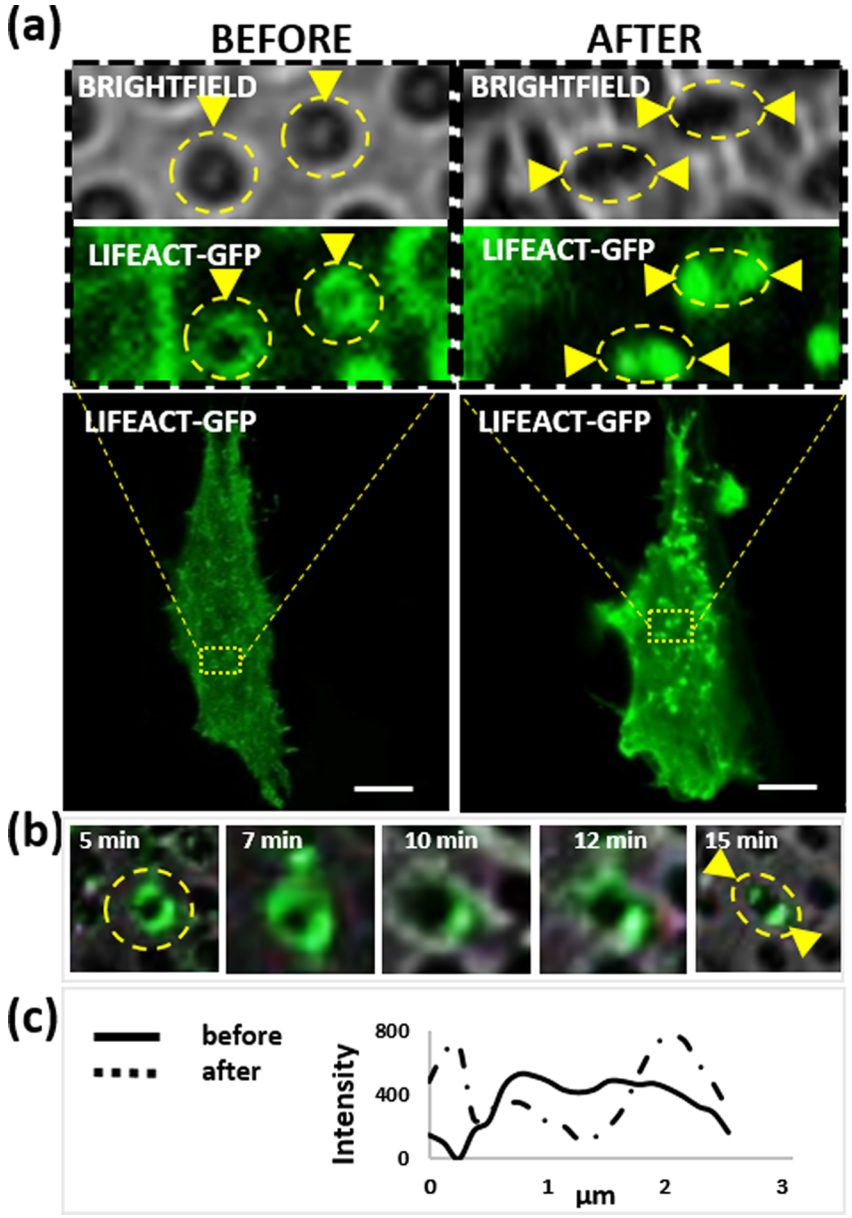

Figure 4. Monitoring curvature-dependent F-actin polymerization in live cells by light-driven reshaping of azostructures. (a) Fluorescence images of U2OS cells expressing Lifeact-GFP before and after ~10 min from azopillar reshaping. The accumulation of F-actin is observed around pillar and at the ends of bars with the high magnification image (dashed circle). (b) High-magnification images of the same azobar at different times show the reorganization of F-actin in response to azostructure reshaping. (c) Intensity profiles of LifeAct-GFP along reshaped pillar, before illumination at 0 min (black line) and 10 min after stimulation (dashed line). The intensity distribution is measured in the same selected ROI and calculated over time with ImageJ.

can further explain the decrease of fluorescence intensity of F-Actin on azobars respect to SiO_2 bars.

Furthermore, we probe the spatial distribution of actin nucleation factor Arp2/3 on azobars and SiO_2 nanobars. Our previous study showed that branched actin was nucleated by the Arp2/3 complex,[16,18,19,47] rather than linear actin, accumulated on nanostructures in a curvature-dependent manner. If branched, actin accumulates at high curvature locations; thus, we expect its nucleation factor also accumulates at the same locations. For this study, U2OS cells were transfected to express Arp3-GFP, a subunit of the Arp2/3 complex. Indeed, we observed an accumulation of Arp3-GFP at the ends of both static SiO_2 nanobars and light-reshaped azobars as shown in Figure 3d. Overall, these results demonstrate that azobars obtained by light-induced reshaping of azopillars are able to induce curvature-dependent recruitment of Apr2/3 and the subsequent polymerization of F-actin similar to static SiO_2 nanobars.

Light-Driven Reshaping of Azostructures Enables Kinetic Measurements of Curvature-Dependent F-Actin Polymerization in Live Cells. The dynamic nature of the light-induced reshaping of azopolymer structures allows kinetic measurements of curvature-dependent F-actin polymerization. For this measurement, we cultured cells for 24 h and observed the accumulation of F-actin on azopillars (Figure 4a). Then the 532 nm laser (1.5 mW) was used to induce the azopolymer nanostructure array, reshaping in the presence of live cells. Here, we set a 5 s exposure time as we observed ~100% cell

DOI: 10.1021/acs.nanolett.9b04307
Nano Lett. 2020, 20, 577−584

viability. Longer exposure time results in the ends of neighboring azobars too close to each other, in which case the cell membrane could not fully wrap around individual azobars. Also, phototoxicity clearly increased with exposure time 15 s or longer (Figure S1 in the Supporting Information).

By taking a time series of Lifeact-GFP snapshots of the selected cell, we measure the dynamics of F-actin reorganization after green-light induced azopolymer reshaping. For fluorescence imaging, we used a weak blue light (0.1 mW) that does not cause azopolymer reshaping. Figure 4b shows fluorescence images of LifeAct-GFP around a single azobar at different times after the reshaping. These images clearly demonstrate F-actin transitioning from a ring-like conformation after 5 min to a definitely distributed and preferential accumulation to the bar ends after 15 min. Figure 4c shows the fluorescence intensity plot where Lifeact-GFP along the sidewall and a concurrent increase toward the ends of reshaped pillars around 10 min from topographic reshaping. On average, the F-actin reorganization happens around 10 ± 2 min after the laser-induced deformation. Therefore, dynamic reshaping of azopolymer topography allows us to monitor kinetics of curvature-sensitive actin polymerization in real-time.

In response to abrupt external perturbations, cells exhibit both elastic and viscous behavior influenced by a combination of membrane, actin cortex, and cytoplasm. The membrane response is highly nonlinear, and the time scale ranges from milliseconds to tens of seconds depending on the time scale and the amplitude of the perturbation.[48] The subsequent cytoskeleton reorganization takes longer time. The time scale we observed for actin cytoskeleton remodeling is consistent with previous studies of cellular processes that rely on cytoskeletal remodeling.[49−52]

Conclusion. In this work, we demonstrate the possibility to use light-responsive azopolymer nanostructures to dynamically change membrane curvatures and intracellular curvature-dependent processes in live cells. We note that dynamically modulating membrane curvatures has been previously achieved by pushing or pulling the cell membrane using optical tweezers and atomic force microscopy.[42,43] Compared with optical tweezers or AFM, the azopolymer deformation approach is fundamentally different and has unique advantages. It affords high throughput, easy access, and does not require sophisticated skills or instruments. Using polarized laser beam, we are able to switch pillar to bar shape along the polarization direction, which dynamically modulates the membrane curvature of U2OS cells to activate intracellular curvature-sensing processes. We demonstrate that curvature-dependent F-actin reorganization takes about 10 min after the light-induced azopolyer reshaping. In this work, the photo-responsive property of azopolymer provides unique advantages for dynamically modulating cellular activities.

■ ASSOCIATED CONTENT

Supporting Information

The Supporting Information is available free of charge at https://pubs.acs.org/doi/10.1021/acs.nanolett.9b04307.

Materials and methods; cell viability on azopillars/azobars; membrane curvature modulation on static and dynamic structures (PDF)

■ AUTHOR INFORMATION

Corresponding Authors

*E-mail: bcui@stanford.edu.

*E-mail: francesca.santoro@iit.it.

ORCID

Francesca Santoro: 0000-0001-7323-9504

Bianxiao Cui: 0000-0002-8044-5629

Notes

The authors declare no competing financial interest.

■ ACKNOWLEDGMENTS

We thank Jong Wook Noh for the support of the fabrication process, Dr. Carolyn Bertozzi for the confocal microscope, and Stanford Nanofabrication and Characterization facilities for the use of instrument. This work was supported by NIH R01GM128142.

■ ABBREVIATIONS

pDR1m, poly(dispersed Red 1 methacrylate); PDMS, poly(dimethylsiloxane)

■ REFERENCES

(1) Ventre, M.; Natale, C. F.; Rianna, C.; Netti, P. A. Topographic Cell Instructive Patterns to Control Cell Adhesion, Polarization and Migration. *J. R. Soc., Interface* **2014**, *11* (100), 20140687.

(2) Bettinger, C. J.; Langer, R.; Borenstein, J. T. Engineering Substrate Topography at the Micro- and Nanoscale to Control Cell Function. *Angew. Chem., Int. Ed.* **2009**, *48*, 5406−5415.

(3) Wu, Y.; Yang, Z.; Law, J. B. K.; He, A. Y.; Abbas, A. A.; Denslin, V.; Kamarul, T.; Hui, J. H. P.; Lee, E. H. The Combined Effect of Substrate Stiffness and Surface Topography on Chondrogenic Differentiation of Mesenchymal Stem Cells. *Tissue Eng., Part A* **2017**, *23* (1−2), 43−54.

(4) Brammer, K. S.; Choi, C.; Frandsen, C. J.; Oh, S.; Jin, S. Hydrophobic Nanopillars Initiate Mesenchymal Stem Cell Aggregation and Osteo-Differentiation. *Acta Biomater.* **2011**, *7* (2), 683−690.

(5) Xie, C.; Hanson, L.; Xie, W.; Lin, Z.; Cui, B.; Cui, Y. Noninvasive Neuron Pinning with Nanopillar Arrays. *Nano Lett.* **2010**, *10* (10), 4020−4024.

(6) Persson, H.; Købler, C.; Mølhave, K.; Samuelson, L.; Tegenfeldt, J. O.; Oredsson, S.; Prinz, C. N. Nanowires: Fibroblasts Cultured on Nanowires Exhibit Low Motility, Impaired Cell Division, and DNA Damage (Small 23/2013). *Small* **2013**, *9* (23), 3905.

(7) Sun, J.; Ding, Y.; Lin, N. J.; Zhou, J.; Ro, H.; Soles, C. L.; Cicerone, M. T.; Lin-Gibson, S. Exploring Cellular Contact Guidance Using Gradient Nanogratings. *Biomacromolecules* **2010**, *11* (11), 3067−3072.

(8) Wu, Y.-N.; Law, J. B. K.; He, A. Y.; Low, H. Y.; Hui, J. H. P.; Lim, C. T.; Yang, Z.; Lee, E. H. Substrate Topography Determines the Fate of Chondrogenesis from Human Mesenchymal Stem Cells Resulting in Specific Cartilage Phenotype Formation. *Nanomedicine* **2014**, *10* (7), 1507−1516.

(9) Sniadecki, N. J.; Desai, R. A.; Ruiz, S. A.; Chen, C. S. Nanotechnology for Cell-Substrate Interactions. *Ann. Biomed. Eng.* **2006**, *34* (1), 59−74.

(10) Antonini, S.; Meucci, S.; Parchi, P.; Pacini, S.; Montali, M.; Poggetti, A.; Lisanti, M.; Cecchini, M. Human Mesenchymal Stromal Cell-Enhanced Osteogenic Differentiation by Contact Interaction with Polyethylene Terephthalate Nanogratings. *Biomed. Mater.* **2016**, *11* (4), 045003.

(11) Jung, A. R.; Kim, R. Y.; Kim, H. W.; Shrestha, K. R.; Jeon, S. H.; Cha, K. J.; Park, Y. H.; Kim, D. S.; Lee, J. Y. Nanoengineered Polystyrene Surfaces with Nanopore Array Pattern Alters Cytoskeleton Organization and Enhances Induction of Neural Differentiation of Human Adipose-Derived Stem Cells. *Tissue Eng., Part A* **2015**, *21* (13−14), 2115−2124.

DOI: 10.1021/acs.nanolett.9b04307
Nano Lett. 2020, 20, 577−584

(12) Lavenus, S.; Berreur, M.; Trichet, V.; Pilet, P.; Louarn, G.; Layrolle, P. Adhesion and Osteogenic Differentiation of Human Mesenchymal Stem Cells on Titanium Nanopores. *Eur. Cell. Mater.* **2011**, *22*, 84−96.
(13) Dalby, M. J.; Gadegaard, N.; Tare, R.; Andar, A.; Riehle, M. O.; Herzyk, P.; Wilkinson, C. D. W.; Oreffo, R. O. C. The Control of Human Mesenchymal Cell Differentiation Using Nanoscale Symmetry and Disorder. *Nat. Mater.* **2007**, *6* (12), 997−1003.
(14) Chen, S.; Jones, J. A.; Xu, Y.; Low, H.-Y.; Anderson, J. M.; Leong, K. W. Characterization of Topographical Effects on Macrophage Behavior in a Foreign Body Response Model. *Biomaterials* **2010**, *31* (13), 3479−3491.
(15) Luu, T. U.; Gott, S. C.; Woo, B. W. K.; Rao, M. P.; Liu, W. F. Micro- and Nanopatterned Topographical Cues for Regulating Macrophage Cell Shape and Phenotype. *ACS Appl. Mater. Interfaces* **2015**, *7* (51), 28665−28672.
(16) Zhao, W.; Hanson, L.; Lou, H.-Y.; Akamatsu, M.; Chowdary, P.; Santoro, F.; Marks, J.; Grassart, A.; Drubin, D.; Cui, Y. Nanoscale Manipulation Of Membrane Curvature For Probing Endocytosis In Live Cells. *Nat. Nanotechnol.* **2017**, *12*, 750.
(17) Galic, M.; Jeong, S.; Tsai, F.-C.; Joubert, L.-M.; Wu, Y. I.; Hahn, K. M.; Cui, Y.; Meyer, T. External Push and Internal Pull Forces Recruit Curvature-Sensing N-BAR Domain Proteins to the Plasma Membrane. *Nat. Cell Biol.* **2012**, *14* (8), 874−881.
(18) Lou, H.-Y.; Zhao, W.; Cui, B. Membrane Curvature Dependent F-Actin Polymerization at Nano-Cell Interface. *Biophys. J.* **2018**, *114*, 690a.
(19) Lou, H.-Y.; Zhao, W.; Zeng, Y.; Cui, B. The Role of Membrane Curvature in Nanoscale Topography-Induced Intracellular Signaling. *Acc. Chem. Res.* **2018**, *51* (5), 1046−1053.
(20) Azatov, M.; Sun, X.; Suberi, A.; Fourkas, J. T.; Upadhyaya, A. Topography on a Subcellular Scale Modulates Cellular Adhesions and Actin Stress Fiber Dynamics in Tumor Associated Fibroblasts. *Phys. Biol.* **2017**, *14*, 065003.
(21) Li, X.; Matino, L.; Zhang, W.; Klausen, L.; McGuire, A. F.; Lubrano, C.; Zhao, W.; Santoro, F.; Cui, B. A Nanostructure Platform for Live-Cell Manipulation of Membrane Curvature. *Nat. Protoc.* **2019**, *14* (6), 1772−1802.
(22) Beckwith, K. S.; Cooil, S. P.; Wells, J. W.; Sikorski, P. Tunable High Aspect Ratio Polymer Nanostructures for Cell Interfaces. *Nanoscale* **2015**, *7* (18), 8438−8450.
(23) Lou, H.-Y.; Zhao, W.; Li, X.; Duan, L.; Powers, A.; Akamatsu, M.; Santoro, F.; McGuire, A. F.; Cui, Y.; Drubin, D. G.; et al. Membrane Curvature Underlies Actin Reorganization in Response to Nanoscale Surface Topography. *Proc. Natl. Acad. Sci. U. S. A.* **2019**, *116* (46), 23143−23151.
(24) Dipalo, M.; McGuire, A. F.; Lou, H.-Y.; Caprettini, V.; Melle, G.; Bruno, G.; Lubrano, C.; Matino, L.; Li, X.; De Angelis, F.; et al. Cells Adhering to 3D Vertical Nanostructures: Cell Membrane Reshaping without Stable Internalization. *Nano Lett.* **2018**, *18* (9), 6100−6105.
(25) Gopal, S.; Chiappini, C.; Penders, J.; Leonardo, V.; Seong, H.; Rothery, S.; Korchev, Y.; Shevchuk, A.; Stevens, M. M. Porous Silicon Nanoneedles Modulate Endocytosis to Deliver Biological Payloads. *Adv. Mater.* **2019**, *31* (12), No. e1806788.
(26) Beckwith, K. S.; Ullmann, S.; Vinje, J.; Sikorski, P. Influence of Nanopillar Arrays on Fibroblast Motility, Adhesion, and Migration Mechanisms. *Small* **2019**, *15* (43), No. e1902514.
(27) Zhao, W.; Hanson, L.; Lou, H.-Y.; Akamatsu, M.; Chowdary, P. D.; Santoro, F.; Marks, J. R.; Grassart, A.; Drubin, D. G.; Cui, Y.; et al. Nanoscale Manipulation of Membrane Curvature for Probing Endocytosis in Live Cells. *Nat. Nanotechnol.* **2017**, *12* (8), 750−756.
(28) Higgins, S. G.; Becce, M.; Seong, H.; Stevens, M. M. Nanoneedles and Nanostructured Surfaces for Studying Cell Interfacing. In *International Conference on the Development of Biomedical Engineering in Vietnam*; Springer, 2018; pp 209−212.
(29) Pirani, F.; Angelini, A.; Frascella, F.; Rizzo, R.; Ricciardi, S.; Descrovi, E. Light-Driven Reversible Shaping of Individual Azopolymeric Micro-Pillars. *Sci. Rep.* **2016**, *6*, 31702.
(30) Wang, W.; Yao, Y.; Luo, T.; Chen, L.; Lin, J.; Li, L.; Lin, S. Deterministic Reshaping of Breath Figure Arrays by Directional Photomanipulation. *ACS Appl. Mater. Interfaces* **2017**, *9* (4), 4223−4230.
(31) Pirani, F.; Angelini, A.; Frascella, F.; Descrovi, E. Reversible Shaping of Microwells by Polarized Light Irradiation. *Int. J. Polym. Sci.* **2017**, *2017*, 1.
(32) Kong, X.; Wang, X.; Luo, T.; Yao, Y.; Li, L.; Lin, S. Photomanipulated Architecture and Patterning of Azopolymer Array. *ACS Appl. Mater. Interfaces* **2017**, *9* (22), 19345−19353.
(33) Cojocariu, C.; Rochon, P. Light-Induced Motions in Azobenzene-Containing Polymers. *Pure Appl. Chem.* **2004**, *76*, 1479−1497.
(34) Bandara, H. M. D.; Dhammika Bandara, H. M.; Burdette, S. C. Photoisomerization in Different Classes of Azobenzene. *Chem. Soc. Rev.* **2012**, *41*, 1809−1825.
(35) Yadavalli, N. S.; Loebner, S.; Papke, T.; Sava, E.; Hurduc, N.; Santer, S. A Comparative Study of Photoinduced Deformation in Azobenzene Containing Polymer Films. *Soft Matter* **2016**, *12*, 2593−2603.
(36) Lee, S.; Kang, H. S.; Ambrosio, A.; Park, J.-K.; Marrucci, L. Directional Superficial Photofluidization for Deterministic Shaping of Complex 3D Architectures. *ACS Appl. Mater. Interfaces* **2015**, *7*, 8209−8217.
(37) Lee, S.; Shin, J.; Lee, Y.-H.; Fan, S.; Park, J.-K. Directional Photofluidization Lithography for Nanoarchitectures with Controlled Shapes and Sizes. *Nano Lett.* **2010**, *10*, 296−304.
(38) Kang, H. S.; Lee, S.; Park, J.-K. Monolithic, Hierarchical Surface Reliefs by Holographic Photofluidization of Azopolymer Arrays: Direct Visualization of Polymeric Flows. *Adv. Funct. Mater.* **2011**, *21*, 4412−4422.
(39) Pirani, F.; Angelini, A.; Ricciardi, S.; Frascella, F.; Rizzo, R.; Ferrarese Lupi, F.; De Leo, N.; Boarino, L.; Descrovi, E. Tunable Hydrophobicity Assisted by Light-Responsive Surface Micro-Structures. *Laser-based Micro- and Nanoprocessing XI* **2017**, 100920A DOI: 10.1117/12.2251008.
(40) Oscurato, S. L.; Borbone, F.; Maddalena, P.; Ambrosio, A. Light-Driven Wettability Tailoring of Azopolymer Surfaces with Reconfigured Three-Dimensional Posts. *ACS Appl. Mater. Interfaces* **2017**, *9*, 30133−30142.
(41) Pirani, F.; Angelini, A.; Ricciardi, S.; Frascella, F.; Descrovi, E. Laser-Induced Anisotropic Wettability on Azopolymeric Micro-Structures. *Appl. Phys. Lett.* **2017**, *110*, 101603.
(42) Nussenzveig, H. M. Cell Membrane Biophysics with Optical Tweezers. *Eur. Biophys. J.* **2018**, *47* (5), 499−514.
(43) Haase, K.; Pelling, A. E. Investigating Cell Mechanics with Atomic Force Microscopy. *J. R. Soc., Interface* **2015**, *12* (104), 20140970.
(44) Schaumann, E. N.; Tian, B. Actin-Packed Topography: Cytoskeletal Response to Curvature. *Proc. Natl. Acad. Sci. U. S. A.* **2019**, *116* (46), 22897−22898.
(45) Rianna, C.; Rossano, L.; Kollarigowda, R. H.; Formiggini, F.; Cavalli, S.; Ventre, M.; Netti, P. A. Dynamic Cell Substrates: Spatio-Temporal Control of Dynamic Topographic Patterns on Azopolymers for Cell Culture Applications (Adv. Funct. Mater. 42/2016). *Adv. Funct. Mater.* **2016**, *26*, 7743.
(46) Rianna, C.; Rossano, L.; Kollarigowda, R. H.; Formiggini, F.; Cavalli, S.; Ventre, M.; Netti, P. A. Spatio-Temporal Control of Dynamic Topographic Patterns on Azopolymers for Cell Culture Applications. *Adv. Funct. Mater.* **2016**, *26* (42), 7572−7580.
(47) Hanson, L.; Zhao, W.; Lou, H.-Y.; Lin, Z. C.; Lee, S. W.; Chowdary, P.; Cui, Y.; Cui, B. Vertical Nanopillars for in Situ Probing of Nuclear Mechanics in Adherent Cells. *Nat. Nanotechnol.* **2015**, *10*, 554−562.
(48) Kollmannsberger, P.; Fabry, B. Linear and Nonlinear Rheology of Living Cells. *Annu. Rev. Mater. Res.* **2011**, *41* (1), 75−97.
(49) Fung, T. S.; Ji, W.-K.; Higgs, H. N.; Chakrabarti, R. Two Distinct Actin Filament Populations Have Effects on Mitochondria,

DOI: 10.1021/acs.nanolett.9b04307
Nano Lett. 2020, 20, 577−584

with Differences in Stimuli and Assembly Factors. *J. Cell Sci.* **2019**, *132* (18), jcs234435.
(50) Chierico, L.; Joseph, A. S.; Lewis, A. L.; Battaglia, G. Live Cell Imaging of Membrane/Cytoskeleton Interactions and Membrane Topology. *Sci. Rep.* **2015**, *4*, 6056.
(51) Fritzsche, M.; Fernandes, R. A.; Chang, V. T.; Colin-York, H.; Clausen, M. P.; Felce, J. H.; Galiani, S.; Erlenkämper, C.; Santos, A. M.; Heddleston, J. M.; et al. Cytoskeletal Actin Dynamics Shape a Ramifying Actin Network Underpinning Immunological Synapse Formation. *Sci. Adv.* **2017**, *3* (6), No. e1603032.
(52) Lee, S.-L.; Nekouzadeh, A.; Butler, B.; Pryse, K. M.; McConnaughey, W. B.; Nathan, A. C.; Legant, W. R.; Schaefer, P. M.; Pless, R. B.; Elson, E. L.; et al. Physically-Induced Cytoskeleton Remodeling of Cells in Three-Dimensional Culture. *PLoS One* **2012**, *7* (12), No. e45512.

DOI: 10.1021/acs.nanolett.9b04307
Nano Lett. 2020, 20, 577−584